PROCEEDINGS OF SPIE REPRINT

SPIE—The International Society for Optical Engineering

Reprinted from

26th AIPR Workshop

Exploiting New Image Sources and Sensors

15–17 October 1997
Washington, D.C.

SPIE PROCEEDINGS SERIES

Volume 3240

Application of the wavelet based Radon transform

Stanley R. Deans and Deepak Gangadharan

University of South Florida, Department of Physics
4202 E. Fowler Avenue, Tampa, FL 33620-5700

ABSTRACT

The theory of the Radon transform forms the foundation for problems of reconstruction from projections. For example, in computerized tomography (CT) the raw data can be identified with the Radon transform of the image. The desired image is found by applying the inverse Radon transform to the projection data. In cases where it is desired to image a local region that is small in comparison to the entire image there is a problem due to the nature of the global properties of the inverse Radon transform in two dimensions. From a practical point of view this means we must have projection data for regions that are not in the region of interest (ROI) in order to stabilize the inversion process that yields the ROI. Introduction of the wavelet transform as an intermediate part of the inversion leads to an important improvement in this procedure. It is possible to devise algorithms such that significantly less radiation exposure is required without causing a noticeable degradation of the image in the ROI. The key is to make use of wavelets with several vanishing moments and to do appropriate sparse sampling away from the ROI. A review of Radon transform inversion is discussed for three major inversion algorithms, and a brief summary of wavelets is given. The current situation on wavelet based Radon transform inversion is reviewed along with potential applications to CT, limited angle CT, and single photon emission computed tomography (SPECT).

KEYWORD LIST

Radon transform, wavelet transform, reconstruction, projections, backprojection, local tomography

1. THE RADON TRANSFORM

Let the function $f(x, y)$ be defined on some domain $D \in \mathbb{R}^2$ of a plane. The Radon transform[1–4] of f is the mapping defined by all possible line integrals of f along lines L that pass through the domain D. We can represent this operation by

$$\check{f} = \mathcal{R}f = \int_L f(x, y)\, ds\,,$$

where ds is an increment of length along L. This mapping and its inverse was studied by Johann Radon[5] in 1917. He showed that if f is continuous with compact support, then $\check{f}$ is uniquely determined by integrating along all lines L. In practical cases the domain is finite and by scaling can be confined to a unit circle. If the plane is associated with a cross section of a physical object, then the line integral represents the integral of some physical characteristic of the object. In CT the object is usually some region of a human body and the characteristic parameter is the linear attenuation coefficient. The line integral can be determined by measuring the attenuation of x-rays passing through the object.

It is useful to associate the line integrals with some coordinate system. One possibility is to place the origin of the coordinate system somewhere near the center of the cross section and describe the location of the line integral by an angle and a distance as illustrated in Fig. 1. For continuous p and ϕ the Radon transform of the function f is given by

$$\check{f}(p, \phi) = \int_{-\infty}^{\infty}\int_{-\infty}^{\infty} f(x, y)\, \delta(p - x\cos\phi - y\sin\phi)\, dx\, dy\,. \tag{1}$$

Note that the delta function picks out the line $p = x\cos\phi + y\sin\phi$ in the xy plane. For a fixed angle the values of the line integrals (projections) as a function of the distance p constitute a profile of the object. The projection profiles are usually measured for incremental values of the angle ϕ and the collection of these constitute a sampling or approximation of the Radon transform.

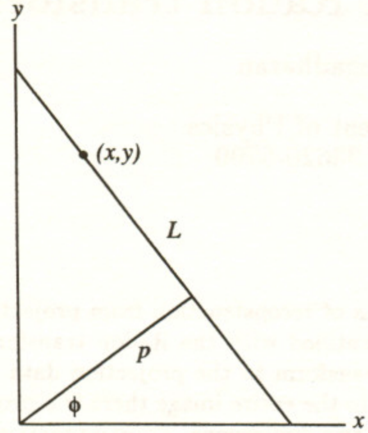

Figure 1. Coordinates in feature space used to define the Radon transform.

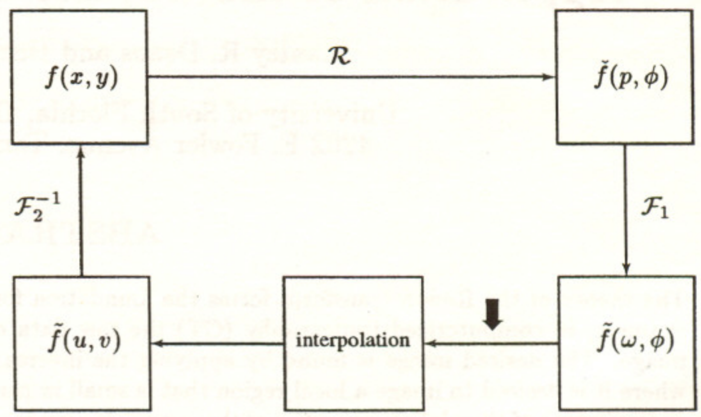

Figure 2. Direct Fourier method.

2. INVERSION

The inversion of the Radon transform to get back the original function is often referred to as the reconstruction problem. The inversion of the Radon transform poses some interesting problems. Any physical method of collecting data, for example by passing a beam of x-rays through tissue, is only an approximation of a line integral. Also this approximation of the line integral is only done at a finite number of angles. Thus any method of reconstruction can at best be an approximation of the original distribution.

2.1 Direct Fourier method

The Fourier slice theorem, also called the projection-slice theorem, provides the connection that relates three spaces, Feature space f, Radon space $\check{f}$, and Fourier space $\tilde{f}$. The theorem states that the one-dimensional Fourier transform of a parallel projection is equal to a slice of the two-dimensional Fourier transform $\tilde{f}$ of the original object f; that is, for each angle ϕ

$$\tilde{f}(\omega,\phi) = \int_0^\infty \check{f}(p,\phi)\, e^{-j2\pi\omega p}\, dp \,. \tag{2}$$

This theorem provides a method for inverting the Radon transform, illustrated in Fig. 2. We can construct a radial grid of the one-dimensional Fourier transforms of the projections. Since only a finite number of projections are taken, we know the values of the function $\tilde{f}$ only along a finite number of radial lines. It is necessary to interpolate from these radial points to points on a rectangular or square grid. The function $\tilde{f}(u,v)$ on this square grid can then be inverted using the inverse two-dimensional Fourier transform. This yields an approximation of the original image $f(x,y)$. In theory, it is possible to determine the grid points of a $N \times N$ matrix provided we have N^2 values of the function $\tilde{f}$ along a finite number of radial lines. This calculation involves solving a large number of simultaneous equations often leading to unstable solutions. A more common method of finding the values on the square grid is to do some kind of nearest neighbor or linear interpolation from the radial points. Since the density of the radial points becomes sparser as one gets farther away from the center, interpolation errors also become larger. This error causes some image degradation due to the greater error in calculating the high frequency components.

This method of inversion is conceptually the easiest to understand, but as things stand now it is difficult to implement. This is partly due to the interpolation and partly due to the two-dimensional Fourier inversion.[1-4] It is still an open question just how much this situation can be changed by inclusion of the wavelet transform in this algorithm.

2.2 FBP, convolution

The algorithm currently being used in most applications of tomography is the filtered backprojection algorithm (FBP). As the name implies, there are two steps to the filtered backprojection algorithm, filtering and backprojection. The filtering is done on each projection before the backprojection operation. A more descriptive name might be backprojection of the filtered projections, but conventions cannot be easily changed.

The backprojection operation follows from the Fourier slice theorem by rewriting the inverse Fourier transform in polar coordinates and rearranging the limits of integration. The formula for the inverse Fourier transform of $\tilde{f}$ can be expressed as

$$f(x,y) = \int_{-\infty}^{\infty}\int_{-\infty}^{\infty} \tilde{f}(u,v)\, e^{j2\pi(ux+vy)}\, du\, dv \;=\; \int_{0}^{2\pi}\int_{0}^{\infty} \tilde{f}(\omega,\phi)\, e^{j2\pi\omega(x\cos\phi + y\sin\phi)}\, \omega\, d\omega\, d\phi\,.$$

This integral can written as two integrals by considering ϕ from 0 to π and then from π to 2π. Then, by symmetry and from the property of the delta function

$$f(x,y) = \int_0^{\pi} d\phi \int_{-\infty}^{\infty} d\omega \int_{-\infty}^{\infty} dt\, \tilde{f}(\omega,\phi)|\omega|\, e^{j2\pi\omega t}\, \delta(t - x\cos\phi - y\sin\phi)\,.$$

Now do the integral over ω before the integral over t,

$$f(x,y) = \int_0^{\pi} d\phi \int_{-\infty}^{\infty} dt\, \delta(t - x\cos\phi - y\sin\phi) \int_{-\infty}^{\infty} d\omega\, |\omega|\, \tilde{f}(\omega,\phi)\, e^{j2\pi\omega t}\,.$$

The inverse Fourier transform over ω yields a new function of t and ϕ,

$$f^*(t,\phi) = \int_{-\infty}^{\infty} |\omega| \tilde{f}(\omega,\phi)\, e^{j2\pi\omega t}\, d\omega\,, \tag{3}$$

and the integral over t gives the backprojection operation $\mathcal{B}$ used to recover the desired function

$$f(x,y) = \int_0^{\pi} d\phi \int_{-\infty}^{\infty} dt\, f^*(t,\phi)\, \delta(t - x\cos\phi - y\sin\phi) = \int_0^{\pi} f^*(x\cos\phi + y\sin\phi, \phi)\, d\phi \equiv \mathcal{B}f^*\,. \tag{4}$$

The integral that gives f^* represents a filtering operation where the frequency response of the filter is given by $|\omega|$; hence the name "filtered projection" for f^*. This type of filter is called a ramp filter.

There is an important alternate method for obtaining f^*. Suppose we can find a well-behaved function $c(t)$ such that its Fourier transform approximates $|\omega|$ for

$$|\omega| < \omega_0\,.$$

Now define a filter function $\tilde{c}$ in terms of a window function w in Fourier space

$$\tilde{c}(\omega) = |\omega| w(\omega)\,. \tag{5}$$

This approach works well when $\check{f}$ has no important high-frequency components; equivalently, $\tilde{f}$ is very small for $|\omega| > \omega_0$. Given these conditions, it follows that f^* is given by the inverse Fourier transform

$$f^*(t,\phi) = \mathcal{F}^{-1}\left[|\omega| w(\omega) \tilde{f}(\omega,\phi)\right]. \tag{6}$$

By use of the Fourier convolution theorem it is possible to work directly in signal space before backprojecting,

$$f^*(t,\phi) = \int_{-\infty}^{\infty} \check{f}(p,\phi)\, c(t-p)\, dp = c(p) * \check{f}(p,\phi)\,. \tag{7}$$

The star on the right means convolution. This equation holds for each projection ϕ, thus the reconstruction procedure can be started as soon as the first projection is measured. We refer to convolution (7) or multiplication (5) in the Fourier domain as a filter. These operations are summarized in Fig. 3.

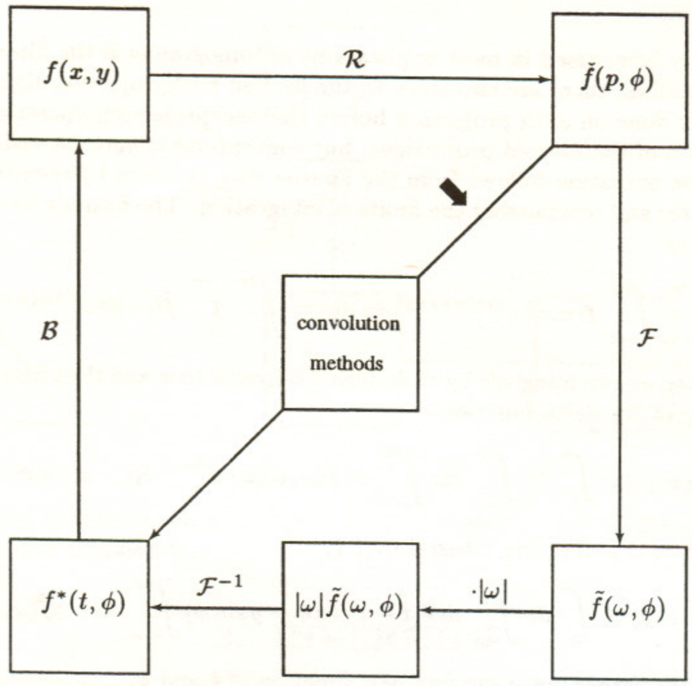

Figure 3. Filtered backprojection, convolution.

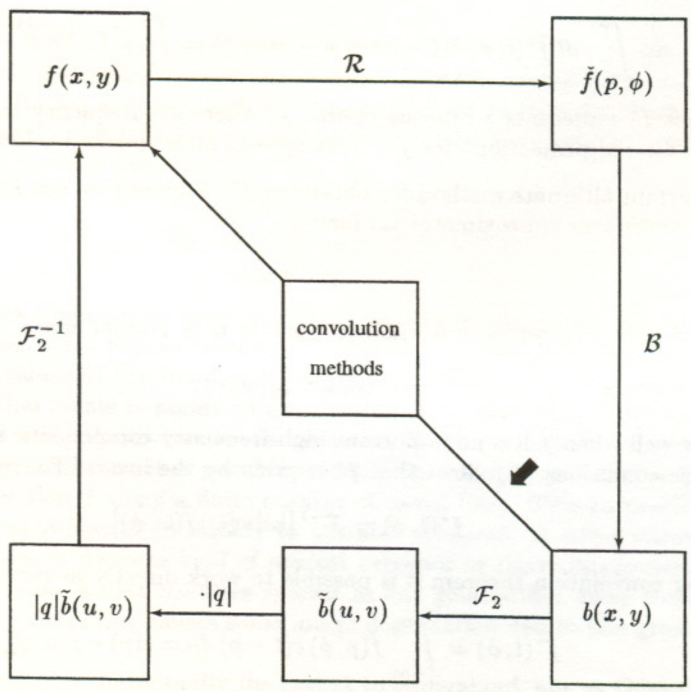

Figure 4. Filter of backprojections.

2.3 Filter of backprojections

It is possible to devise an algorithm where the backprojection operation comes immediately after obtaining the projections. This method is called the filter of backprojections, illustrated in Fig. 4. Note that the path along the bottom of the figure involves a 2-D Fourier transform and the final path to $f(x,y)$ a 2-D inverse Fourier transform. It follows from the Fourier convolution theorem that the convolution path is a 2-D filtering operation. The filter function $\tilde{c}$ and the window function w are functions of two variables,

$$\tilde{c}(u,v) = |q|w(u,v)\,, \qquad q = \sqrt{u^2+v^2}\,. \tag{8}$$

Now the last part of the path to $f(x,y)$ in Fig. 4 is given by

$$f(x,y) = \mathcal{F}_2^{-1}\left[\tilde{c}\,\tilde{b}\right] = c(x,y) ** b(x,y)\,. \tag{9}$$

This method requires a two-dimensional convolution. One of the attractive features is that the filter function can be computed in advance and transformed to give

$$c(x,y) = \mathcal{F}_2^{-1}\tilde{c}(u,v)\,. \tag{10}$$

This means that the inversion process can begin immediately upon calculating the backprojections $b(x,y)$. Thus, the real-time computational load, which is still considerable, involves calculating the backprojection and a 2-D convolution.

3. LOCALITY

The reason for introducing the window function is related to the fact that the inverse Fourier transform of $|\omega|$ is not locally supported. This relates to the lack of differentiability at the origin. It is this non-local behavior that leads to the need for global values of the Radon transform even when trying to reconstruct a local region.

Another way to see this is from the formula for f^* in terms of a Hilbert transform,[1-4]

$$f^*(t,\phi) = \frac{-1}{2\pi}\mathcal{H}\frac{\partial\check{f}(p,\phi)}{\partial p}\,, \tag{11}$$

where the Hilbert transform of a function g is given by

$$\mathcal{H}g = \frac{1}{\pi}\int_{-\infty}^{\infty}\frac{g(p)}{p-t}\,dp\,.$$

Differentiation is a local operation but the Hilbert transform is not, since it imposes a discontinuity upon the Fourier transform of any function with average value not zero, and discontinuities on the higher derivatives which are not zero at the origin. Discontinuities at the origin in the frequency domain spread the support of the functions in the time domain. A local basis function will not remain local after filtering. However, the spreading of the support of the function *will not occur* if the function's Fourier transform is zero at the origin, and the function has many zero moments. Further, one can construct functions with only a few zero moments whose support is essentially unchanged by the Hilbert transform.[6]

Wavelets are generally constructed with as many zero moments as possible, given other constraints such as locality and smoothness.[7] The more zero moments, the smoother the wavelet; however, wavelets with a large number of vanishing moments have a broader region of support that may be undesirable. Some sort of compromise is appropriate. The local properties of the high resolution components of a wavelet transform will remain local after filtering. This property makes the inclusion of wavelets in reconstruction algorithms very attractive. For example, if each projection is expanded using a rather smooth wavelet basis, it is possible to essentially localize the Hilbert transform, and stabilize the filtered backprojection algorithm. In other words, wavelet bases with sufficiently many zero moments have essentially the same region of support after the ramp filtering as before. This is the main reason why the wavelet transform is useful for finding stable local solutions to the inversion problem.

4. WAVELETS

For details on wavelets we refer the reader to standard sources.[7–9] For our purposes here it is sufficient to assume a multiresolution analysis along with wavelet functions and scaling functions.

Let the scaling function (often called the father wavelet) be designated by the usual notation $\phi(x)$ and the wavelet function (the mother wavelet) by $\psi(x)$. These functions have compact support and have the properties that $\int \phi(x)\,dx = 1$ and $\int \psi(x)\,dx = 0$ where the integral is over the region of support. The basis functions are defined in terms of father and mother wavelets,

$$\phi_{j,k}(x) = 2^{-j}\phi(2^{-j}x - k)\,, \qquad \psi_{j,k}(x) = 2^{-j}\psi(2^{-j}x - k)\,, \qquad j,k \in \mathbb{Z}\,. \tag{12}$$

These basis functions are scaled (index j) and translated (index k) versions of the father and mother wavelets. By construction, they satisfy orthogonality conditions

$$\int \phi_{J,k}\,\phi_{J,k'}\,dx = \delta_{k,k'} \qquad \int \psi_{j,k}\,\psi_{j',k'}\,dx = \delta_{j,j'}\,\delta_{k,k'} \qquad \int \psi_{j,k}\,\phi_{J,k'}\,dx = 0\,.$$

A measure of the scale is given by 2^j. There are several families of wavelets; some of the more popular ones are designated by Haar, Daublets, Symmlets, and Coiflets.[7–9] The last three of these families contain subfamilies with an increasing degree of smoothness. Once the family is selected a table of filter coefficients can be used in a very efficient algorithm to find the wavelet coefficients required for the wavelet decomposition of some function $f(x)$. For a continuous function the orthogonal series approximation is given by

$$f(x) \approx \sum_k d_{1,k}\psi_{1,k}(x) + \sum_k d_{2,k}\psi_{2,k}(x) + \ \ldots\ + \sum_k d_{J,k}\psi_{J,k}(x) + \sum_k s_{J,k}\phi_{J,k}(x)\,. \tag{13}$$

Here J is the number of scales (multiresolution components), and k ranges from 1 to the number of coefficients for the corresponding J. The s coefficients are the "smooth" coefficients, representing a very coarse approximation to f. The d coefficients are the "detail" coefficients. They represent the fine to coarse resolution of f as j goes from 1 to J. If $f(x)$ is sampled at a discrete number of points, say 2^J, then the expansion (13) is exact and there are 2^J transform values.

Example: A simple example may be useful. Suppose the function f is sampled at $n = 2^J$ points; for purposes of this example $2^4 = 16$ points. There are $n/2 = 8$ coefficients $d_{1,k}$ at the finest scale, $n/4 = 4$ coefficients $d_{2,k}$ at the next scale, $n/8 = 2$ coefficients $d_{3,k}$ at the next scale, $n/16 = 1$ coefficient $d_{4,k}$ at the coarsest scale, and $n/16 = 1$ smooth coefficient $s_{J,k}$. This gives a grand total of $8 + 4 + 2 + 1 + 1 = 16$ coefficients. There is an inverse transform that carries the 16 transformed values back to the original data set exactly.

All of this is important for inclusion with the Radon transform for several reasons. The projection data are discrete, and are over a finite region. An appropriate discrete wavelet transform with compact support can be used to represent the projection data exactly. Both the Radon and wavelet transforms are linear transformations. Very fast wavelet transform algorithms (of order n) exist. These are faster than FFT algorithms that go as $n \log n$. Features that have a characteristic scale will show up strong in the multiresolution decomposition at the same scale, and will be essentially ignored at other scales.

A multiresolution wavelet decomposition also holds for functions $f(x, y)$ defined in a plane. One way to do this is to take tensor products of horizontal and vertical 1-D wavelets. This leads to four basic types of 2-D wavelets, in an obvious notation where s, h, v, and d refer to smooth, horizontal, vertical, and diagonal,

$$\begin{aligned}
\Phi^s(x,y) &= \phi_h(x)\phi_v(y)\\
\Psi^h(x,y) &= \psi_h(x)\phi_v(y)\\
\Psi^v(x,y) &= \phi_h(x)\psi_v(y)\\
\Psi^d(x,y) &= \psi_h(x)\psi_v(y)\,.
\end{aligned} \tag{14}$$

The concepts of smooth and detail remain, with Φ^s associated with the smooth part of the image. The horizontal, vertical, and diagonal detail parts are associated with Ψ^h, Ψ^v, and Ψ^d. Decompositions for 2-D images similar to (13) in 1-D exist, and there are fast transforms for the analysis and synthesis. At each resolution level J there are four parts as indicated above. The three Ψ parts are saved. To go the the next level the Φ^s part is decomposed into four more parts. This procedure is repeated as far as needed or until no more data exists. If there are 2^J points then it is possible to go to J levels. For further discussion, see some of the standard sources,[7–9] in particular, Chapter 10 of Daubechies,[7] for illustrations.

5. RADON PLUS WAVELETS

There are several ways to insert a wavelet expansion in some part of the inversion process for the reconstruction problem. For early work on combining Radon and wavelet transforms see Walnut[10] and Berenstein and Walnut[11] and references therein. Here we review some possibilities developed by several research groups for the reconstruction methods discussed earlier. Although good progress has been made, it still remains a research problem to evaluate fully these techniques from a practical and clinical perspective. Also, it is very likely that there are ways, yet to be discovered, for combining Radon transforms and wavelets.

5.1 Wavelets and FBP

The filtered backprojection (FBP) algorithm is the most popular algorithm for reconstruction and has received most attention in connection with use of wavelets. One possibility is to apply the 1-D wavelet transform to the projections at each angle. Wavelets are introduced at the point indicated by the black arrow in Figure 3. This corresponds to expanding $\check{f}(p, \phi)$ in a series like (13) for each projection angle. Olson and DeStefano[6] developed an algorithm of this type. Their algorithm can be used to reduce radiation exposure when the region of interest (ROI) is small compared with the total area of the transverse section to be reconstructed. The ROI is exposed just as in conventional cases, but there is reduced exposure throughout the region away from the ROI. This works because the low resolution wavelet coefficients can be approximated by angular interpolation between neighboring full projections. This is followed by an inverse wavelet transform and a standard FBP algorithm. Their method seems to work well in the ROI, but it can produce very bad results away from the ROI.

An entirely different approach to a wavelet based FBP algorithm is taken by Delaney and Bresler.[12] They base their algorithm on a full 2-D separable discrete dyadic wavelet transform of the reconstructed image. Imagine a separate Fig. 3 for each multiresolution image associated with the components Φ^s, Ψ^h, Ψ^v, and Ψ^d. The projections are subjected to a full 2-D multiresolution decomposition. The standard FBP algorithm is modified to have an angle dependent filter. You can see how this can be done by following along the bottom path in Fig. 3. This modified FBP algorithm is used to reconstruct all low resolution wavelet coefficients. The high resolution wavelet coefficients are reconstructed near the ROI. This produces a 2-D wavelet transform of the image. The image is then found by an inverse 2-D wavelet transform. One advantage of this approach is that image processing operations such as noise reduction, edge detection, and compression can be carried out in the wavelet domain before the final reconstruction.

The 2-D wavelet based inversion algorithm developed by Rashid-Farrokhi and collaborators[13] is similar in some respects to the method used by Delaney and Bresler. It makes use of a full 2-D multiresolution decomposition and produces the 2-D wavelet transform of the image. A major difference is the amount of data required away from the ROI. This algorithm uses almost completely local data. Full use is made of the observation that for some wavelet bases with sufficiently many vanishing moments, the ramp-filtered scaling function as well as the wavelet function has very rapid decay. Several basis wavelets have been tried and they get their best results using a biorthonormal basis when the scaling and wavelet functions have essentially the same support after ramp filtering. This leads to an algorithm that has reduced exposure compared with the other algorithms.[6,12] There is no need to obtain global properties by sparsely sampled full exposure projections. They compute a small number of projections on lines passing close to the ROI to take into account the small increase in support of the wavelet and scaling function caused by the ramp filter. Fewer projections are used and there is uniform exposure at all angles. This may be attractive for implementation in practical situations. This algorithm can work on off-center regions of interest, multiple regions, as well as regions that are centered.

5.2 Backprojection followed by wavelets

The algorithm illustrated in Fig. 4 can be used to form a wavelet based inversion algorithm. One possibility is to introduce a full 2-D wavelet transform following the backprojection of the projections. The location is indicated by the black arrow in Fig. 4. An algorithm of this type has been developed by Kolaczyk[14] using the wavelet-vaguelette decomposition created by Donoho.[15] After the vaguelette coefficients are found for each resolution level and direction, a denoising method known as wavelet shrinkage[16] is applied. This serves as a method of regularization for the ill-posed inversion problem. After this procedure the inverse 2-D wavelet transform is applied to obtain the reconstructed image.

5.3 Direct Fourier and wavelets

The direct Fourier method is not a popular method of reconstruction, although conceptually it is the most straightforward method. Most of the problem comes from the need to perform an interpolation in Fourier space prior to implementation of the inverse 2-D Fourier transform. This problem is currently under investigation by the authors. The idea is to introduce the wavelet transform at the location of the black arrow in Fig. 2 and make use of wavelet regularization methods. The technique has promise, but it still needs a full evaluation and comparison with other methods.

6. POTENTIAL

Combining the Radon and wavelet transforms clearly has potential in CT when there is a need to image a local region, and there is no concern about the region away from the ROI. There are other situations where introduction of wavelets may be useful. One case is the limited angle CT problem. Some of the techniques used for calculating wavelet coefficients away from the ROI may carry over to situations where it is impossible to obtain a complete set of projections. Another case is with single photon emission computed tomography (SPECT). In SPECT noise is especially bothersome. Some of the denoising methods used in wavelet analysis may be helpful. Another possibility is to use wavelet techniques in SPECT for edge enhancement, along with denoising.

7. REFERENCES

1. S. R. Deans, *The Radon Transform and Some of its Applications*, Wiley, New York, 1983. Revised edition, Krieger, Malabar, FL, 1993.
2. S. R. Deans, "Radon and Abel transforms," in *The Transforms and Applications Handbook*, A. D. Poularikas, ed., pp. 631-717, CRC Press, Roca Raton, FL, 1996.
3. A. C. Kak and M. Slaney, *Principles of Computerized Tomographic Imaging*, IEEE Press, New York, 1988.
4. F. Natterer, *The Mathematics of Computerized Tomography*, Wiley, New York, 1986.
5. J. Radon, "Über die Bestimmung von Funktionen durch ihre Integralwerte längs gewisser Mannigfaltigkeiten," *Berichte Sächsische Akademie der Wissenschaften. Leipzig, Math-Phys. Kl.*, **69**, 262–267, 1917.
6. T. Olson and J. DeStefano, "Wavelet localization of the Radon transform," *IEEE Trans. Signal Processing*, **42**, 2055–2067, 1994.
7. I. Daubechies, *Ten Lectures on Wavelets*, SIAM, Philadelphia, PA (1992).
8. M. Vetterli and J. Kovačević, *Wavelets and Subband Coding*, Prentice-Hall, Englewood Cliffs, NJ, 1995.
9. A. Bruce and H.-Y. Gao, *Applied Wavelet Analysis with S-PLUS*, Springer, New York, 1966.
10. D. Walnut, "Applications of Gabor and wavelet expansions the the Radon transform." in *Probabilistic and Stochastic Methods in Analysis, with Applications*, J. Byrnes, et al. eds., pp. 187–205, Kluwer Academic Publishers, The Netherlands, 1992.

11. C. A Berenstein and D. Walnut, "Local inversion of the Radon transform in even dimensions using wavelets." in *75 Years of Radon Transform*, S. Gindikin and P. Michor, eds., pp. 45–69, International Press, Cambridge, MA, 1994.

12. A. H. Delaney and Y. Bresler, " Multiresolution tomographic reconstruction using wavelets", *IEEE Trans. on Image Processing*, **4**, 799–813, 1995.

13. F. Rashid-Farrokhi, K. J. R. Liu, C. A. Berenstein, and D. Walnut, "Wavelet-based multiresolution local tomography," to appear: *IEEE Trans. on Image Processing*, October, 1997.

14. E. D. Kolaczyk, "A wavelet shrinkage approach to tomographic image reconstruction," *J. Amer. Stat. Assoc.*, **91**, 1079–1099, 1996.

15. D. L. Donoho, "Nonlinear solution of linear inverse problems by wavelet-vaguelette decomposition," *Applied and Computational Harmonic Analysis*, **2**, 101–126, 1995.

16. D. L. Donoho and I. M. Johnstone, "Ideal spatial adaptation via wavelet shrinkage," *Biometrica*, **81**, 425–455, 1994.